Experimental study on properties of hybrid stable & surfactant-free nanofluids GNPs/CNCs (Graphene nanoplatelets/cellulose nanocrystal) in water/ethylene glycol mixture for heat transfer application

M. Sandhya [a,*], D. Ramasamy [a], K. Kadirgama [b, c], W.S.W. Harun [a] , R. Saidur [d,e]

[a] College of Engineering, University Malaysia Pahang, 26300 Gambang, Pahang, Malaysia

[b] Faculty of Mechanical and Automotive Engineering Technology, Universiti Malaysia Pahang, 26600 Pekan, Pahang, Malaysia

[c] Automotive Engineering Centre, Universiti Malaysia Pahang, 26600 Pekan, Malaysia

[d] Research Centre for Nano-Materials and Energy Technology (RCNMET), School of Science and Technology, Sunway University, Malaysia

[e] Department of Engineering, Lancaster University, Lancaster, LA1 4YW, UK

Abstract:

The heat transfer capacity of any thermal cooling system depends on two factors, i.e., the selection of the coolant and the geometrical pattern of the approach. This article summarizes nanofluids' preparation ranging from 0.01 % to 0.2 % using Graphene nanoplatelets & CNC dispersed in a base fluid. The combination of water with ethylene glycol (EG) is a form of customary heat transmit liquids regularly utilized in numerous energy practices to maintain the water's decent cooling (or heating) capability; thus, 60:40 ratio of EG: W mixture used as the base fluid for thermo-physical properties enhancements. These nanofluids prepared are not used with surfactants as it results in generating bubbles and contaminating the heat transfer channels, influencing the overall performance. XRD & FESEM techniques were used to analyze the surface. The

investigated nanofluids remained stable, with no substantial sedimentation for 30 days. The results of GNPs/CNC nanofluids at 0.1% volume concentration has proper stability showing excellent colloidal stability in the base fluid of EG: W at a ratio of 60:40. The present hybrid nanofluid has the ability to switch the traditional heat transfer fluids leading to efficient & compact thermal structures.

Keywords: Graphene nanoplatelets (GNP's), Cellulose nanocrystals (CNC), Hybrid nanofluid, Preparation, Stability.

1.0 Introduction:

Nanofluids have been found vital; nanofluids have emerged as a significant participant in heat transfer applications [1]. For the time being, more research is needed on hybrid nanofluids before they can be put to use in the manufacturing environment. They may have been used in virtually every area of heat transfer technology [2]. It has increasingly been known that traditional working fluids (such as water, engine oil, and ethylene glycol) have poor heat transfer capability in various engineering processes (such as heating or cooling processes, power production, and chemical processes). As a result, using ultrafine solid particles dispersed in the base fluid as a means of improving the thermal performance of these fluids was a novel suggestion [3-5]. Even though early research revealed that using particles of sizes in millimetres or micrometres in solutions improved performance, obstacles such as low suspension stability and resulting clogging of flow channels were encountered [6, 7]. Nanosized particle suspensions (1–100 nm) in a conventional base heat transfer fluid (named "nanofluid") exhibited improved stability, better rheological properties, and much higher thermal conductivities than a millimetre or micrometre-sized particle suspensions [8].

In 1995, Choi was the first person to use the term "Nanofluid." The suspension of solid nanoparticles in a base fluid, on the other hand, does not produce a simple combination and still has an instability problem; consequently, the stability of nanofluid should be thoroughly researched [9, 10]. There are numerous ways to improve the stability of nanofluids [11-15]. Surfactants, on the other hand, are thought to be the simplest and most cost-effective way to minimize sedimentation and improve the stability of nanoparticles in aqueous media.

Several published studies in the previous few years have drawn academics' attention to the subject of carbon nanostructure-based nanofluids. The use of carbon nanotubes was the main focus of researchers in this subject [16], single-walled carbon nanotubes [17], double-walled carbon nanotubes [18], multi-walled carbon nanotubes [19], graphene oxide [20], Graphene [21], graphene nanoplatelets [22], and hybrid [23] to prepare nanofluids [24-25]. Because of its remarkable mechanical, physical, thermal, and electrical properties, Graphene has attracted plenty of attention [26, 27]. On the other hand, Graphene nanoplatelets combine the advantages of monolayer graphene, such as high surface area and good heat conductivity, with the advantages of highly complex graphitic carbon, such as high stability and low cost. GNPs, on the other hand, tend to aggregate due to the strong Van der Waals relations that result from the high specific surface area [28-30]. As a result, dispersion stability should be thoroughly explored for the effective use of GNPs in the nanofluid area [11]. The author produced dispersions with a volume content of 0.5–4% GNPs in ethylene glycol as a base fluid. Intensive ultrasonication and no functionalization were used by Lee and Rhee [22]. A thermal conductivity reproducibility test confirmed the stability of the nanofluids. Using covalent and non-covalent functionalization, some researchers developed water-based GNP nanofluids with weight concentrations of 0.025 %, 0.05 %, and 0.1 % [11]. Carboxyl groups and SDBS surfactants were used to make covalently and non-

covalently functionalized GNPs, respectively. All of the nanofluids produced had a viscosity greater than that of water [31]. In addition, nanofluids with non-covalently functionalized GNPs had a higher viscosity than those with covalent functionalization, attributable to the SDBS surfactant's presence.

In the literature, a wide range of nanoparticles and base fluids have been studied. Among the materials studied, carbon-based nanostructures have proven to be particularly promising. From carbon black [32] to graphite [33], as well as carbon nanostructures, e.g. single, multiwall and functionalized nanotubes [33], carbon nano horns [34], several nanofluids having nanoparticles of carbon allotropes have been analyzed for solar energy applications. Graphene is one of the most captivating carbon allotropes [35]. Graphene nanoplatelets or nanosheets are little flakes made up of multiple layers of pinned Graphene that have some of the same excellent qualities as Graphene but at a cheaper cost of manufacture. The dispersion of reasonably large graphene nanoplatelets in water for solar applications is described in the literature [36-37].

However, in order to produce a better dispersion process in most aqueous or organic solvents, it is crucial to chemically change the (hydrophobic) graphene surface, in addition to reducing particle sizes as much as feasible., e.g., by oxidation [38] or functionalization by a polycarboxylate chemical alteration, as in the case of the nanoparticles studied in this study. This investigation demonstrates the novel approach toward hybrid nanofluids by employing nanoparticles as Graphene nanoplatelets and crystal nanocellulose for improved thermal conductivity of coolants in thermal applications. CNCs are nanosized natural biopolymers; however, CNCs thermal properties, crucial for future applications as automated resources, are less investigated. This research aimed to study the analysis, materials, and equipment used to characterize the nanofluids

for water & ethylene glycol (EG)-based Graphene nanoplatelets (GNPs) & hybrid nanoparticles, followed by investigation on stability.

2.0. Materials and methods

2.1. Materials

Graphene nanoplatelets (GNPs) with a specific surface area (SSA) of 800 m^2/g have been used in this study are obtained from Nanografi nanotechnology (Turkey) with specifications; purity: 99.9 %, size: 3 mm, diameter: 1.5 μm. At the same time, crystalline nanocellulose was purchased from MY Biomass Sdn. Bhd. Malaysia. Due to its hydrophilic nature, extracting CNC in powder form from the obtained pulp was difficult. For CNC processing in powder form, a spray drying procedure with a small blower was used. The moisture in the pulp or suspensions was swiftly evaporated when they came into contact with hot air, which flowed through the spray dryer's nozzle opening and created a stable CNCs flake. CNC flakes were obtained and pulverized into powder form.

2.2. Preparation of nanofluid

The required Graphene nanoplatelets & CNC nanofluid was successfully prepared in the Advanced Automotive Liquid Lab of the Faculty of Mechanical Engineering, University Malaysia Pahang. GNPs with different volume concentrations of 0.01%, 0.05%, 0.1%, & 0.2% were weighed using the internal sartorius analytical balance (Model: BSA224S-CW) followed by magnetic stirring and scattering in ethylene glycol/distilled water solution at a ratio of 60:40 for about 2-3 hours. Ultrasonication was carried out using an ultrasonication probe (CE ISO Ultrasonic Homogenizer

Sonicator Processor Cell Disruptor Mixer 20-1000mL) with an output power of 900 W and a power supply frequency range 20KHz with a probe diameter of φ13mm [28, 39].

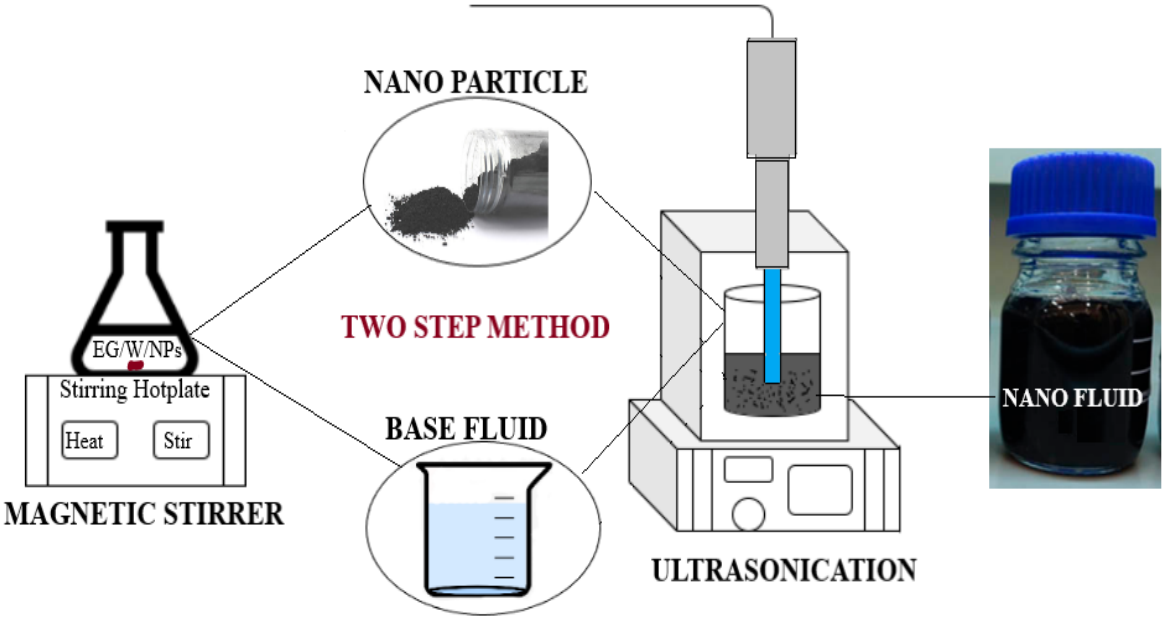

Figure 1: Preparation of nanofluid by a Two-step method

Carbon-based nanoparticles cannot be sustainably distributed in base fluid in the absence of a surfactant due to their hydrophobic nature. It was investigated that GNPs can be dispersed without surfactants in a medium having stirrer & probe sonication. Ultrasonication was carried out for 5 hours in order to disperse and stabilize the nanoparticles properly. Similarly, hybrid nanofluid preparation includes GNPs and CNCs at a ratio of 50:50 is dispersed via magnetic stirring in Ethylene Glycol-distilled water (60:40) base fluid for about 2-3 hours 5 hours ultrasonication process with a power output of 50%. During the sonication process, after every 15 minutes, an interval gap of 5 mins was taken to avoid the nanofluid overheating up related to particles' properties. The below Figure 1 shows the schematic representation of preparing nanofluid. By using equation (2), the density of nanoparticles was confirmed for hybrid nanoparticles.

2.3. Characterization of nanofluid

2.3.1. Stability measurements

Because of nanoparticles wide surface area, they agglomerate and disrupt the stability of hybrid nanofluids, which is a crucial criterion for their use. On this basis, the stability and dispersibility of nanofluids with the addition of GNP: CNC nanoparticles were investigated using the sedimentation method with pictures taken at various times, UV–Vis spectroscopy, and Zeta potential analysis. UV-vis spectroscopy analysis was performed using PerkinElmer's LAMBDA™ UV/Vis with UV-spectrometer operational array of wavelengths 200– 800 nm using particular quartz cuvettes suitable for measurement of light absorbance for all the samples to record the spectra. All samples were diluted in base fluid for proper light transmission across them. The Zeta potential of the nanofluids prepared was measured by Zeta potential Anton Paar lite sizer 500. The Zeta potential measurement shows the degree of repulsion among close particles of the identical charge in nanofluid dispersion. Thermogravimetric analysis (TGA) was used to assess the thermal stability of all prepared nanofluids from 30 °C to 500 °C at a raging rate of 10 °C min^{-1} in N_2 using the TA Instrument (Perkin Elmer TGA 4000, USA).

2.3.2. Physicochemical Characterization

Transmission Electron Microscope (TEM) works for the microstructural characterization of nanofluids. A digital TEM was used to determine the dispersion and particle size measurement of EG-water based GNPs & hybrid GNPs nanofluids. The nanofluid samples were sonicated for 15 min before TEM analysis. The nanofluid solution composed of GNPs and CNC of the nano-base fluid and evaluated with a 200 KV voltage by the TEM device (Tecnai G2 20 S-TWIN, USA) with an accelerating voltage of 200 KV. X-ray diffraction (XRD) was conducted for the GNPs and CNC

nanofluids using a (Rigaku D/MAX-2500PC, Japan) diffractometer with Cu Kα radiation (λ = 1.54056 Å) at 40 KV and 30 mA, with a scan rate of 0.02˚/s. X-ray Diffraction (XRD) analysis was used to examine phase assessment of the nanoparticle. For microstructure characterization, the prepared nanofluid samples are coated to analyze the superficial morphology. While the dispersion of nanoparticles in the fluid was analyzed using (SEM) scanning electron microscopy (HITACHI/TM 3030 PLUS, Czech Republic). The FTIR spectrometer simultaneously gathers luminous data over a broad spectral scale. FTIR analysis was carried out to investigate the nature and interaction of the functional groups. The spectrums of the nanofluids were noted between 4000 – 500 cm^{-1} frequencies to detect the chemical composition of functional groups with KBr by making pallets of compounds.

2.3.3 FESEM microscopy

The structure of formed filaments was observed using field emission scanning electron microscopy (FESEM, Zeiss Sigma HD VP, Germany) at 0.5 kV acceleration voltage. All samples were sputtered with platinum prior to observation. Samples morphologically examined the as-received powder sputtered with platinum before observation using a FESEM to capture topographical images [27, 40].

3. Results and discussion

3.1. Nanofluid preparation

The process of preparation used for graphene nanoplatelets and hybrid nanoparticles dispersion is a two-step method of preparation. The required Graphene & nanocellulose hybrid nanofluid was successfully prepared in the Advanced Automotive Liquid Lab (A2LL) of the Faculty of Mechanical Engineering, University Malaysia Pahang. The Ultrasonication method is the most

influencing method for engendering highly stable GNPs and hybrid nanoparticles dispersion over an ultrasonication time of 5 hours [27-28, 41]. High ultrasonication time was adopted to break the nanoparticles and subsequent dispersion into the base fluid without the ease of surfactant with different concentrations ranging from 0.01%, 0.05%, 0.1%, 0.2%. Characterization and stability of the as-prepared nanofluids were studied. From an operational standpoint, nanofluid stability analysis is one of the essential factors in its successful implementation [42]. At the same time, the best sample was chosen in terms of long-term stability. The parameters such as concentration, the requisite volume of nanofluid and amount of GNP and CNC to be mixed with the base fluid were estimated and concluded before the preparation. Weights of nanoparticles were confirmed using equation (1). The volume of GNP and CNC were determined by using Equations (1) and (2).

$$W_{\text{G-CNC}} = \left(\frac{\varphi}{100-\varphi}\right) \times \left(\frac{\rho\, G-C}{\rho\, BF}\right) W_{\text{bf}} \qquad \text{Equation (1)}$$

$$\rho_{\text{G-CNC}} = \frac{\varphi_{\text{G}}\rho_{\text{G}} + \varphi_{\text{CNC}}\,\rho_{\text{CNC}}}{\varphi_{\text{total}}} \qquad \text{Equation (2)}$$

Where,

φ means the volume concentration of nanofluids,

W is the weight, and

ρ determines the density.

The subscripts G & CNC are the nanoparticles and bf represent base fluid, respectively.

3.2. X-ray diffraction

A diffraction pattern is created whenever X-rays interact with a crystalline substance (phase). The XRD can be described as a fingerprint of the substance because a similar pattern evolved for the same substance, either analyzed as a single substance or present in the mixture of substances. In a mixture of substances, each gives its pattern independently of the others. Figure 1 shows diffraction peaks at 2θ =15.7259°, 22.8375°, 34.6054° and 26.3514°, 43.9549°, 54.1401° belonging to CNC and graphene diffraction planes, respectively. The peak at 2θ=26.3514° in Graphene represented a typical diffraction pattern for graphitic carbon [15, 43-45].

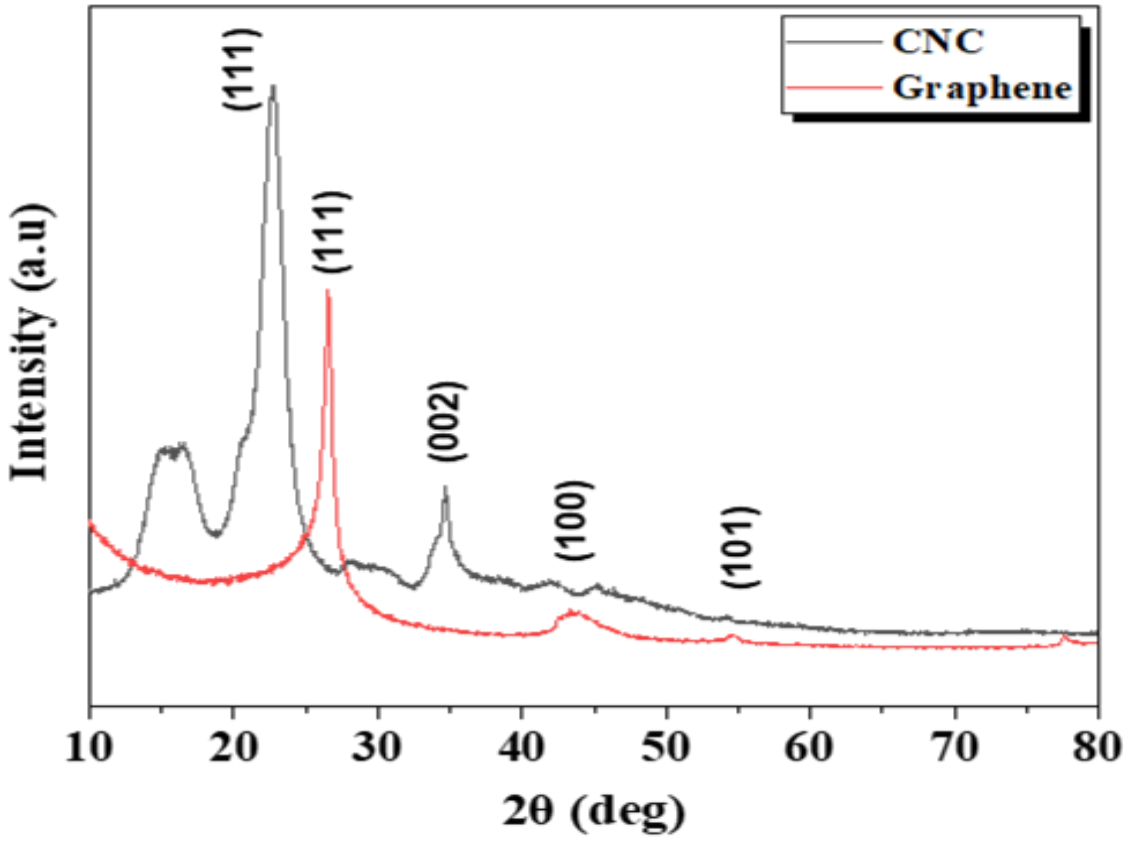

Figure 2: XRD analysis of CNC and Graphene nanoplatelets nanoparticles.

Furthermore, a negatively diffracted peak at 22.8375° demonstrated the linked carbon in cellulosic form. It can also be seen in Figure 2 that the intensity of the peak in CNC is stronger than the

198 graphene peak. It could be explained that Graphene Nanoplatelets' amount and quality increased
199 at higher reaction temperatures. Adequate pre-intercalation to weaken the resistance force and
200 intensified bubble generation to increase driving force via temperature manipulation is essential
201 for highly efficient graphite exfoliation [46].

202

203 **3.3. Macrostructure characterization**

204 SEM (scanning electron microscopy) examines the material's topographic, crystalline,
205 composition, and morphology. Sample preparation was done by adding a consecutive drop (2 to 3
206 drops) of nanofluid on a clean glass slide and dried in the oven at 60° C followed by platinum
207 coating. A scanning electron microscope analyzes a specimen with a beam of electrons to create
208 an amplified object image. Electrons from the beam collide with the object's surface and come
209 back. These dispersed electrons are detected and converted into an image. In the current research,
210 SEM was used to photograph the surface analysis of the dispersion of the nanoparticles in the base
211 fluids. Particle dispersion of Graphene and CNC was photographed at various magnifications, as
212 shown in Figure 3.

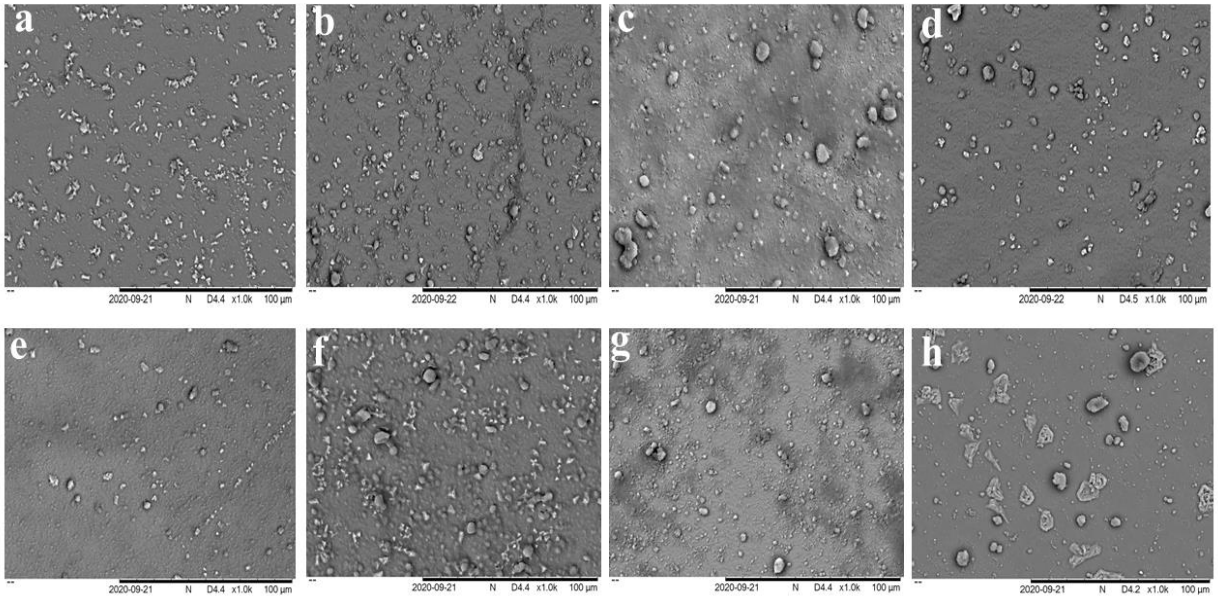

Figure 3: SEM images of Graphene nanoplatelets & hybrid nanoparticles in base fluid at different volume concentrations (a) G 0.01% (b) G 0.05% (c) G 0.1% (d) G 0.2% (e) G+CNC 0.01% (f) G+CNC 0.05% (g) G+CNC 0.1% (h) G+CNC 0.2 %

Figure 3 (a-d) represents the uniform distribution of GNPs in the base fluid. While upon deep observation small degree of agglomeration can see as concentration increases from 0.05% to 0.2%. Figure 3 (e-h) represented the surface chemistry of hybrid nanofluid with an agglomeration pattern towards higher concentration. Agglomeration can be described mainly due to improper mixing of temperature effect causing hybrid nanoparticles to coalesce [47]. Furthermore, the Figure supports the rising shift of GNPs in base fluids (EG/Water), i.e., 0.01% GNPs-EG/W nanofluid showing less amount (Figure 3a) and 0.20% GNPs-EG/W nanofluid showing the high amount. Dispersion of nanoparticles in the base fluid is a critical step. The prepared nanofluid should be an agglomerate-free, stable suspension [48].

3.3 Thermogravimetric (TGA) analysis

TGA is an analytical technique for determining a material's thermal stability and the percent of volatile substances by measuring the weight change while a sample is heated. The weight is recorded as a function of increasing temperature and is generally conducted in air or an inert gas, such as Helium or Argon. The measurement is sometimes done in a lean oxygen atmosphere ((1 to 5) percent O_2 in N_2 or He) to slow oxidation. TGA measurement was carried out for all GNP/GNP: CNC-EG/W nanofluids with distinct volume concentration by verifying the sample mass loss through heating in the temperature range of 30 °C to 500 °C and obtained results are shown in Figure 4. There is different weight loss observed for GNPs and GNP+CNCs as we can observe from the below image that from 100 °C -200 °C there is a weight loss displayed at ramps around 130 °C for G (0.01-0.2) & G+CNC (0.01-0.05%) while at the ramp around 150 °C for CNC (0.1-0.2%) attributed mainly to loss of moisture contents. When the volume concentration of GNP and GNP: CNC nanoparticles increases, the degradation temperature shifts to the upper side. The change in the TGA curve shows that adding nanoparticles to nanofluids allows them to survive higher temperatures than the base fluid (i.e., EG/W). The final weight loss at 200 °C was attributed to the removal of oxygen-containing groups. This could also be ascribed to the high-water repulsive nature of Graphene Nanoplatelets and Cellulose Nano Crystals. In addition, the weight change in an air atmosphere is typically a superposition of the weight loss due to oxidation of carbon into gaseous carbon dioxide and the weight gain due to oxidation of residual metal on the catalyst [49-51].

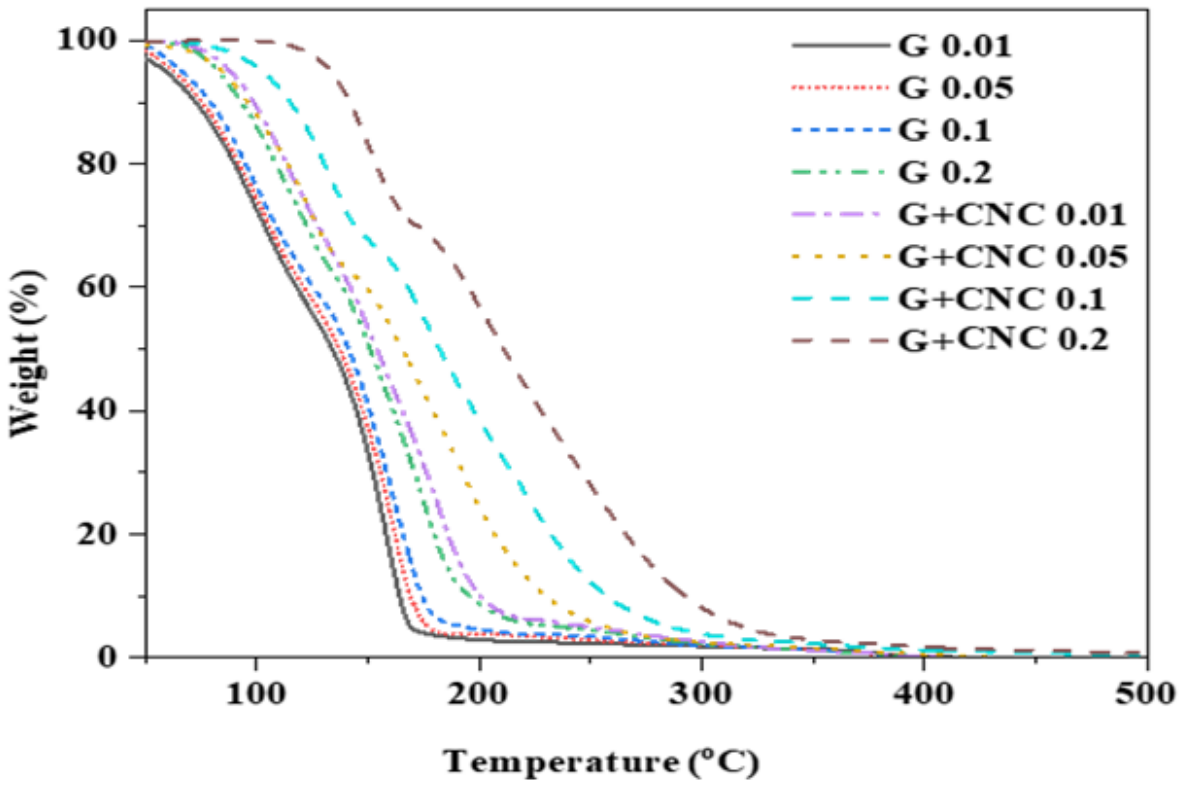

Figure 4: Nanofluid Weight (%) vs Temperature(˚C) graph for TGA analysis

3.4 FTIR

The chemical composition of single and hybrid nanofluids was investigated using FTIR spectra, and the results are displayed in Figure 5 for various ratios of graphene nanoplatelets and CNC. For CNCs, typical signals from cellulose functional groups occurred. Typical O-H stretching vibrations are seen at 3400 cm^{-1}, whereas symmetrical and antisymmetric C-H stretching vibrations are noticed at 2900 cm^{-1}, and C-H scissoring, and rocking vibrations are seen at 1500–1300 cm^{-1} and 760–720 cm^{-1}, respectively [52]. Bending vibrations of adsorbed moisture create the sharp peak at 1640 cm^{-1}, whereas C-H scissoring bending is responsible for the band at 1450 cm^{-1} [53]; this generally has a lower intensity than microcrystalline cellulose, indicating that

intermolecular hydrogen bonds have been disrupted [54]. Finally, the C-O stretching of ether groups accounts for the bandwidth from 1150 to 1000 cm^{-1} [55]. When compared to raw cellulose, certain bands in CNC nanoplatelets faded, indicating that the dissolution process significantly impacts crystallinity [56]. The existence of a new band in the amorphous area at 990 cm^{-1}, related to C-O stretching, verified this behaviour, implying that the transition from cellulose happened throughout the breakdown and regeneration phases [57]. The signal at 1655 and 1550 cm^{-1}, attributed to the stretching of carboxyl and aromatic groups of GNPs, respectively, confirms the existence of GNP in the adsorbent and is the main difference between cellulose and cellulose-GNP spectra [58]. As additives, CNC nanoparticles did not cause any undesirable reaction pathways. Based on this discussion, it may be determined that no chemical interaction between various materials has occurred, which may result in a significant change in chemical or functional bonding.

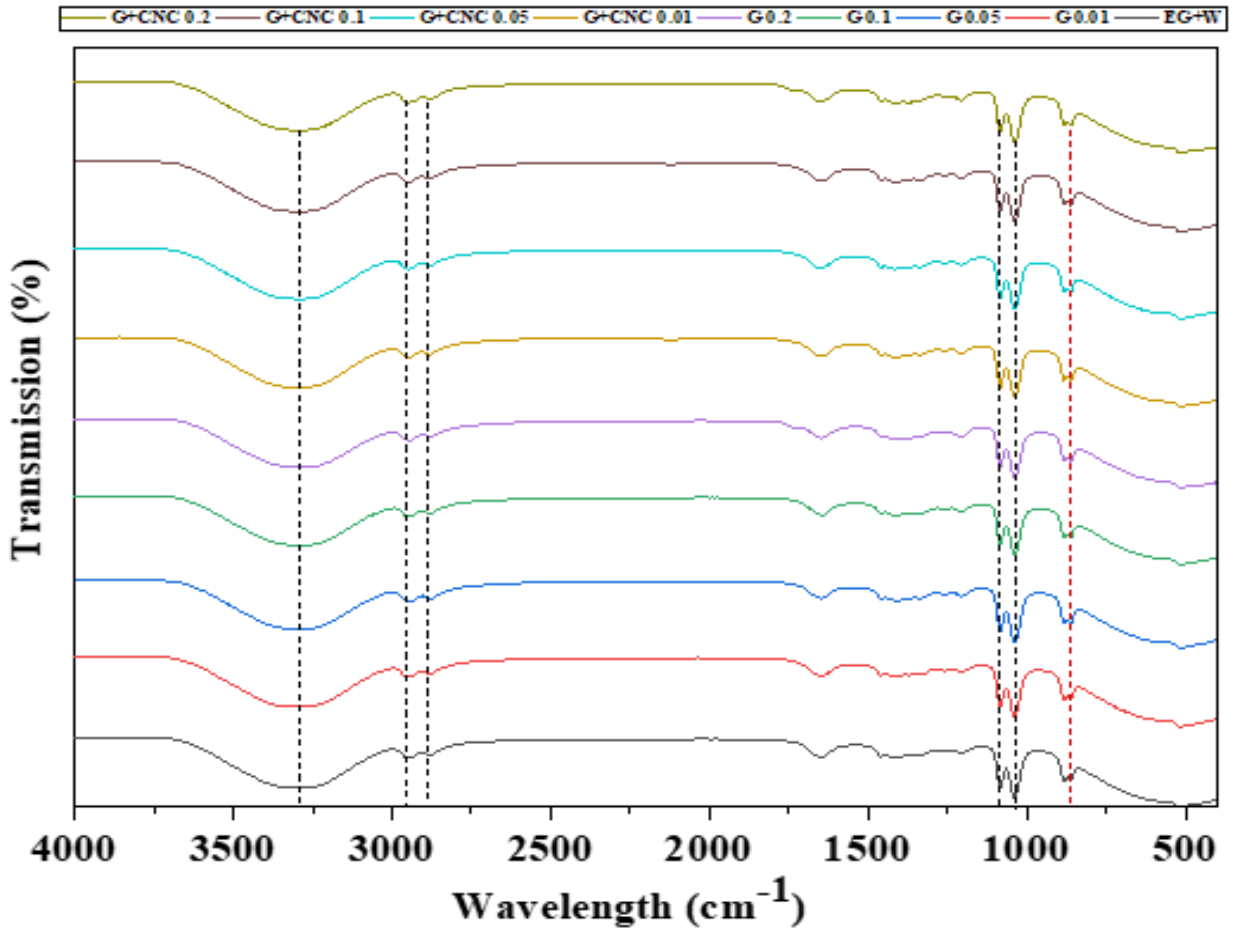

Figure 5: FTIR analysis for various ratios of graphene nanoplatelets and GNPs/CNC.

3.5. Field Emission Scanning Electron Microscopy (FESEM)

Figure 6 (a & b) represented the FESEM images for GNP and CNC. A uniform dendrite type irregular shape can be seen for GNPs, as represented in Figure 6(a). The bulk of the particles, as can be seen in the image, have a platelet structure. The agglomerated particles of GNPs are 100-500nm range. At the same time, CNC showing a porous microstructure with a flower type arrangement. A uniform porous microstructure layered surface morphology can be observed and envisioned the homogeneity and uniformity of different phases as a single hybrid nanofluid [59]. The agglomerated particle range is around 4 µm for CNC. Despite this limitation, image analysis

can provide a general but noticeable assessment. The length of functionalized MWCNT was found to be between 1 and 3µm using FESEM images with reliable length measurements [60].

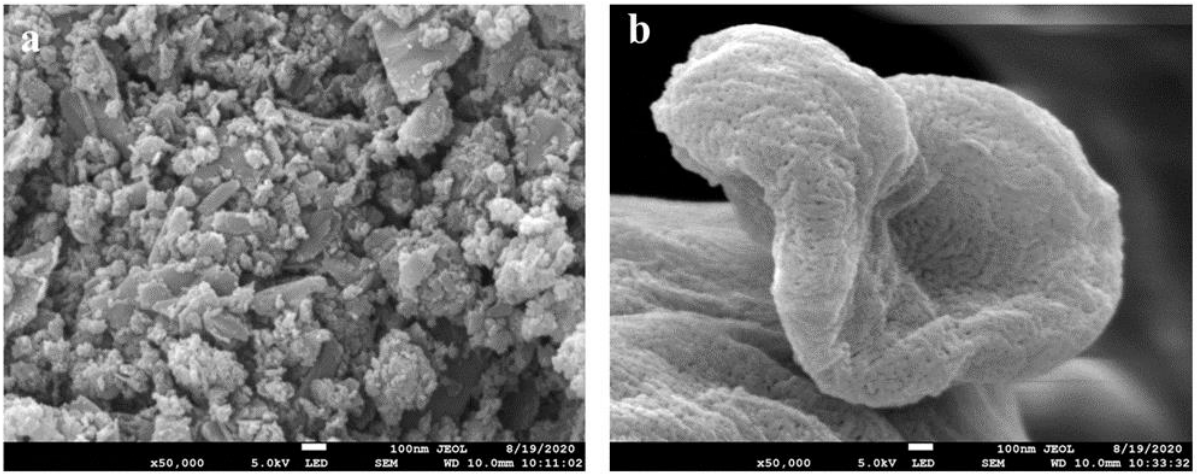

Figure 6: FESEM images of (a) Graphene nanoplatelets (b) CNC nanoparticles.

3.6. Transmission electron microscopy (TEM) (Morphological analysis)

To determine the size of the nanoparticles, a Transmission Electron Microscopy (TEM) experiment was performed [61]. Figure 7 displays CNC and GNPs nanoparticle shape and dispersion examined by TEM. The various GNPs /CNC (Graphene with crystal nanocellulose nanofluid) images are shown in Figure 7. The transparency in Figure 7(b) suggests well-dispersed GNPs with a CNC matrix. It can be observed from the images that the concentration of the nanoparticles increased, resulting in decreased transparency, indicating the agglomeration. There are low partial aggregates for a 0.1% volume concentration of hybrid nanofluid compared to 0.2% GNPs/CNC nanofluid. The microstructure TEM analysis is studied to understand the dispersion of the Graphene nanoplatelets and Cellulose nanocrystal morphology in the base fluid (EG/W). Figure 7(c) demonstrates as platelet structure of Graphene and CNC exhibiting the fragile structure

behaviour with a clean and smooth surface in the base fluid. In conclusion, the morphology of the scattered GNPs and CNC indicates the excellent preparation and dispersion of the nanoparticles in the base fluid of ethylene glycol and water.

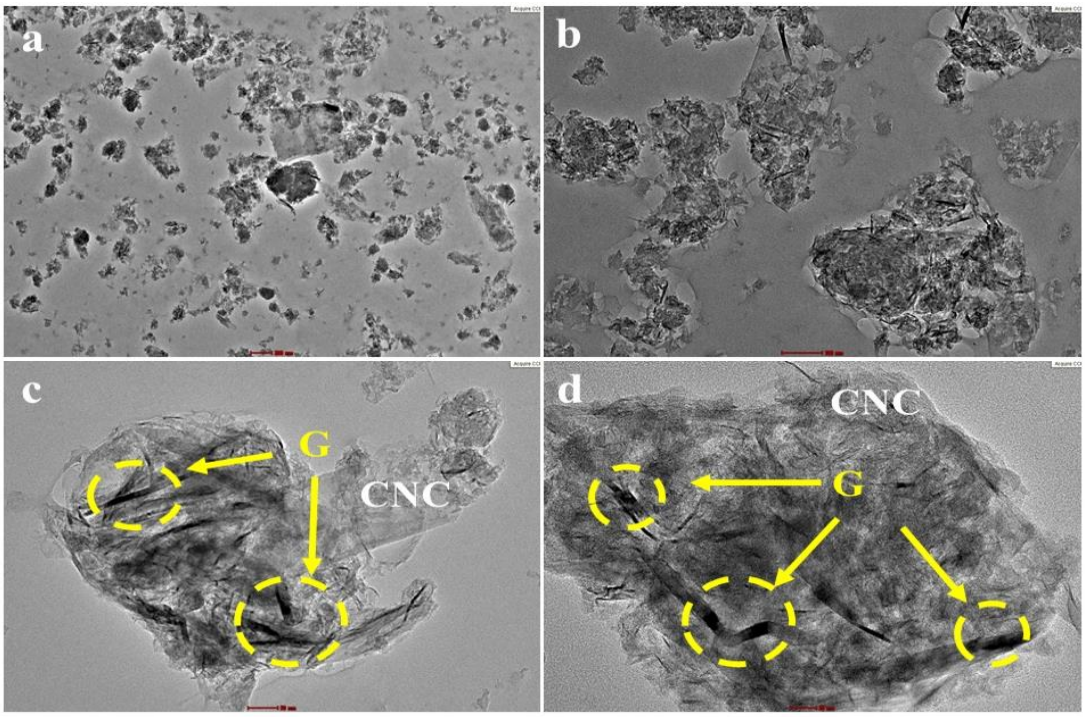

Figure 7: TEM images of prepared nanofluids (a) 0.1% G/CNC at magnification, (b) 0.2% G/CNC at magnification, (c) 0.1%G/CNC at magnification, and (d) 0.2% G/CNC at different magnifications

4. Stability analysis

4.1. Visual observation

GNP tends to remain water repellent and is therefore difficult to disperse in a base fluid because of this hydrophobicity [62]. For this reason, the nanofluids are well prepared and dispersed using

an ultrasonicator, and there was no sedimentation in the sample that was kept for three months before being analyzed. The photographs from Figure 8 show good stability without any sedimentation after 10 days of prepared fluid and even after 60 days of prepared fluid.

Figure 8: Stability test; visual observation (a) after preparation (b) after 10 days (c) 30 days (d) 60 days

4.2 UV-VIS Spectroscopic Analysis

In this study, the sedimentation observation of GNPs/GNPs: CNC nanoparticles with various volume concentrations in EG/W is investigated by UV–vis spectroscopy by recording the spectrums by applying them in the range of wavelengths 200–800 nm [63]. Quartz cuvettes suitable for the UV region were used to determine the light absorbance of all samples at specific time intervals. The UV–vis field for CNC nanoparticles and different dispersed non-covalently

functionalized GNPs. Figure 9(a) shows that the graphene nanoplatelet nanofluid forms can grasp evident illumination in the 200–400 nm wavelength range. Moreover, the quick absorption band at 236nm is correlated with the π-π transition of the C=C bond.

It is clear from this that the peak absorption due to the presence of GNPs in all samples occurs in the wavelength range of 255–269 nm, and that after that peak and within the wavelength range of 255–269 nm, the peak absorption due to the presence of GNPs in all samples occurs in the wavelength range of 255–269 nm as shown in Figure 9 (b), a decline in absorbance was detected in all the trials. For the nanofluid with 0.01, 0.05, 0.10 & 0.2% GNPs/GNPs: CNC volume concentration, a broad absorbance band was clearly visible. Furthermore, it has been discovered that as the GNPs/GNPs: CNC (hybrid) nanoparticle concentration increases, the revealed band location for all samples gets broader. Among all nanofluid concentrations, the UV-Vis spectrums show that 0.20 percent GNPs and GNPs: CNC- EG/W nanofluids had the highest absorption peak, indicating greater nanofluid suspension stability.

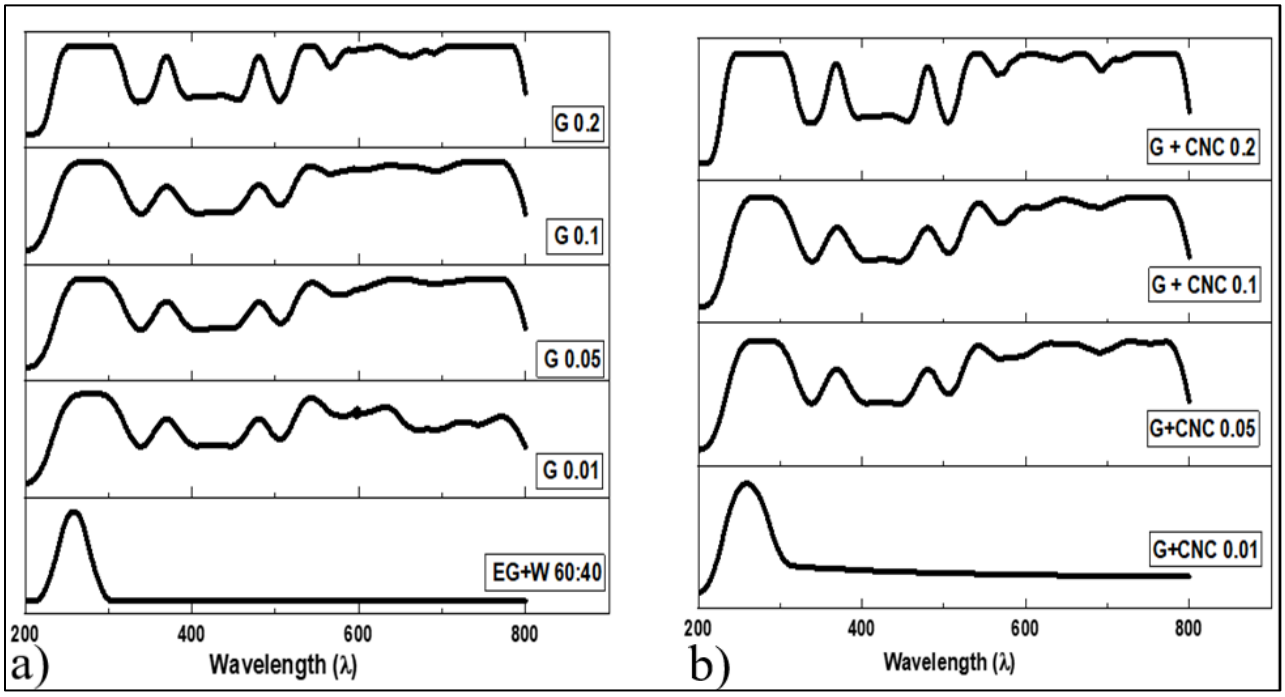

Figure 9 (a & b): UV-Vis analysis of Graphene nanoplatelets and GNPs/CNC nanofluids.

4.3. Zeta potential analysis

The zeta potential is a measure of the repulsive and attractive forces between nanoparticles suspended in liquid, and the magnitude of the zeta potential value can validate the relative stability of the dispersion [64]. The higher the absolute value, the higher the dispersion stability, and the closer the zeta potential is to 0 mV, the higher the degree of aggregation. For instance, nanoparticles in the dispersion are stable when the absolute value of the zeta potential is higher than ±30mV. This zeta potential stability analysis of single and hybrid nanofluids was carried out by measuring the conductivity of the nanoparticles, which measures the potential difference across the boundaries between the solid and the liquid phases (Anton Paar Litesizer 500, Germany) by testing Zeta potential. This is also known as the Z-potential approach, and it is an efficient and common way for assessing the stability of colloidal suspensions. Figure 10 shows the zeta potential measurements to quantitatively characterize the colloidal stability of the Graphene Nanoplatelets & Cellulose Nano Crystal particles in ethylene glycol-water base fluids. The charge on a particle in the shear plane is known as the zeta potential. This surface charge value is helpful for understanding and forecasting particle interactions in suspension. The interface that divides the mobile fluid from the fluid that remains attached to the surface is the electrical potential at the sliding plane [65].

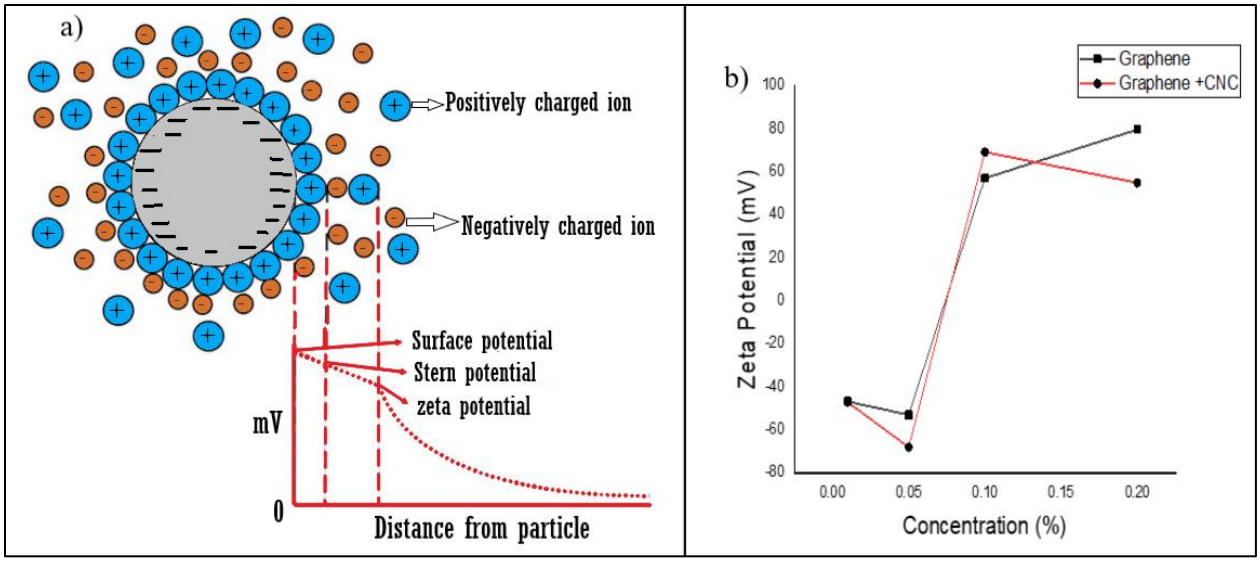

Figure 10: a) Zeta potential diagram, b) zeta potential analysis of Graphene nanoplatelets and GNPs/CNC nanofluids.

Electrokinetic potential in colloidal dispersions is referred to as zeta potential in science terms [66]. The zeta potential was slightly higher with -69 and 79 mV values in the below Figure 10. These values are commonly used to determine if a single or hybrid nanofluid has enough mutual repulsion force to generate a stable aqueous dispersion. Due to electrostatic repulsion, particles having a zeta potential of -30 mV to +30 mV are generally considered stable. Experimentally, it is observed that highest magnitude of zeta potential (ζ) is obtained for 0.2 % graphene platelets nanofluid with 79.62mV, and -46.76 mV, -52.98 mV, & 57.018 mV for 0.01,0.05 &0.1% respectively. Similarly for hybrid nanoparticles nanofluids (GNPs/CNC-EG/W) the maximum magnitude attained at 0.05 & 0.1 % volume concentration with -68.032 mV & 69.192 mV respectively. The observed graphene dispersion results were negative zeta potentials & positive zeta potentials for very stable colloidal solutions. The zeta potential value indicated above shows that Graphene and hybrid Graphene EG/W dispersion exhibit good stability. The particles with a positive zeta potential have a positive charge. Colloids with a high zeta potential (positive or

negative) are stable electrically, whereas colloids with a low zeta potential tend to coagulate or flocculate [67-68].

5. Conclusions

Graphene Nanoplatelets & Cellulose Nano Crystal particles in ethylene glycol-water base fluid dispersion were investigated at various (0.01-0.2) volume % concentrations in preparation and stability analysis for an application of automotive radiator. The results indicated that the mixing ratio of Graphene nanoplatelets and CNC particles in a base fluid (0.01wt. %-0.2wt. %) had the highest change percentage. The results of GNPs/CNC nanofluids at 0.1% volume concentration has proper stability showing excellent colloidal stability in the base fluid of EG: W at a ratio of 60:40. It is observed from the UV-Vis spectrums that among all the concentrations of nanofluids, 0.10% & 0.2% GNPs and GNPs: CNC-EG: W nanoparticles exhibit maximum absorption peak, indicating the better stability of the nanofluid suspension. The TGA analysis revealed that the weight of nanofluid began to decrease at 130 °C temperature and degraded at 500 °C, as the degradation temperature increased by increasing the GNP and GNP: CNC nanoparticles volume concentration. The nanofluids with a volume concentration of 0.20 % GNP: CNC nanoparticles show the most significant shift in degradation temperature compared to the base fluid. At 150 °C, it begins to degrade, and at 500 °C, it entirely decomposes. FTIR findings show no chemical reaction between distinct particles that might significantly change chemical or functional interactions. Finally, it can be concluded that GNPs and CNC nanoparticles can be added to the EG/W base fluid, and this hybrid nanofluid can be prepared with good dispersion stability, which can be used for various applications where this stability gives better thermophysical properties.

Acknowledgements

The authors would like to thank University Malaysia Pahang (UMP) for Grant RDU 190194, FRGS/1/2018/TK03/UMP/02/26, and UMP Flagship RDU192204 for financial assistance and facilities provided. The authors would also like to thank Sunway University for the facilities provided.

Declaration of Competing Interest

The authors declare that they have no known competing financial interests or personal relationships that could have appeared to influence the work reported in this paper.

References

[1] Babu JR, Kumar KK, Rao SS. State-of-art review on hybrid nanofluids. Renewable and Sustainable Energy Reviews. 2017 Sep 1;77:551-65.

[2] Sarkar J, Ghosh P, Adil A. A review on hybrid nanofluids: recent research, development and applications. Renewable and Sustainable Energy Reviews. 2015 Mar 1;43:164-77.

[3] Hetsroni G, Rozenblit R. Heat transfer to a liquid—solid mixture in a flume. International Journal of Multiphase Flow. 1994 Sep 1;20(4):671-89.

[4] Sandhya M, Ramasamy D, Sudhakar K, Kadirgama K, Harun WS. Hybrid nano-coolants in automotive heat transfer–an updated report. Maejo International Journal of Energy and Environmental Communication. (2020);2(3):43-57.

[5] Sohn CW, Chen MM. Microconvective thermal conductivity in disperse two-phase mixtures as observed in a low velocity Couette flow experiment.

[6] Mahian O, Kianifar A, Kalogirou SA, Pop I, Wongwises S. A review of the applications of nanofluids in solar energy. International Journal of Heat and Mass Transfer. 2013 Feb 1;57(2):582-94.

[7] Natarajan E, Sathish R. Role of nanofluids in solar water heater. The International Journal of Advanced Manufacturing Technology. 2009 Jul 1:1-5.

[8] Choi SU, Eastman JA. Enhancing thermal conductivity of fluids with nanoparticles. Argonne National Lab., IL (United States); 1995 Oct 1.

[9] Meibodi ME, Vafaie-Sefti M, Rashidi AM, Amrollahi A, Tabasi M, Kalal HS. The role of different parameters on the stability and thermal conductivity of carbon nanotube/water nanofluids. International Communications in Heat and Mass Transfer. 2010 Mar 1;37(3):319-23.

[10] Sarsam WS, Kazi SN, Badarudin A. A review of studies on using nanofluids in flat-plate solar collectors. Solar Energy. 2015 Dec 1;122:1245-65.

[11] Amiri A, Sadri R, Shanbedi M, Ahmadi G, Chew BT, Kazi SN, Dahari M. Performance dependence of thermosyphon on the functionalization approaches: an experimental study on thermo-physical properties of graphene nanoplatelet-based water nanofluids. Energy conversion and management. 2015 Mar 1;92:322-30.

[12] Amiri A, Shanbedi M, Yarmand H, Arzani HK, Gharehkhani S, Montazer E, Sadri R, Sarsam W, Chew BT, Kazi SN. Laminar convective heat transfer of hexylamine-treated MWCNTs-based turbine oil nanofluid. Energy conversion and management. 2015 Nov 15;105:355-67.

[13] Kumar V, Tiwari AK, Ghosh SK. Application of nanofluids in plate heat exchanger: a review. Energy conversion and management. 2015 Nov 15;105:1017-36.

[14] Shanbedi M, Heris SZ, Amiri A, Hosseinipour E, Eshghi H, Kazi SN. Synthesis of aspartic acid-treated multi-walled carbon nanotubes based water coolant and experimental investigation of thermal and hydrodynamic properties in circular tube. Energy Conversion and Management. 2015 Nov 15;105:1366-76.

[15] Yarmand H, Gharehkhani S, Ahmadi G, Shirazi SF, Baradaran S, Montazer E, Zubir MN, Alehashem MS, Kazi SN, Dahari M. Graphene nanoplatelets–silver hybrid nanofluids for enhanced heat transfer. Energy conversion and management. 2015 Aug 1;100:419-28.

[16] Nasiri A, Shariaty-Niasar M, Rashidi AM, Khodafarin R. Effect of CNT structures on thermal conductivity and stability of nanofluid. International Journal of heat and Mass transfer. 2012 Feb 1;55(5-6):1529-35.

[17] Nanda, J., Maranville, C., Bollin, S. C., Sawall, D., Ohtani, H., Remillard, J. T., & Ginder, J. (2008). Thermal conductivity of single-wall carbon nanotube dispersions: role of interfacial effects. The Journal of Physical Chemistry C, 112(3), 654-658.

[18] Assael MJ, Metaxa IN, Arvanitidis J, Christofilos D, Lioutas C. Thermal conductivity enhancement in aqueous suspensions of carbon multi-walled and double-walled nanotubes in the presence of two different dispersants. International Journal of Thermophysics. 2005 May;26(3):647-64.

[19] Ding Y, Alias H, Wen D, Williams RA. Heat transfer of aqueous suspensions of carbon nanotubes (CNT nanofluids). International Journal of Heat and Mass Transfer. 2006 Jan 1;49(1-2):240-50.

[20] Lee SW, Kim KM, Bang IC. Study on flow boiling critical heat flux enhancement of graphene oxide/water nanofluid. International Journal of Heat and Mass Transfer. 2013 Oct 1;65:348-56.

[21] Yu W, Xie H, Wang X, Wang X. Significant thermal conductivity enhancement for nanofluids containing graphene nanosheets. Physics Letters A. 2011 Mar 7;375(10):1323-8.

[22] Lee GJ, Rhee CK. Enhanced thermal conductivity of nanofluids containing graphene nanoplatelets prepared by ultrasound irradiation. Journal of materials science. 2014 Feb;49(4):1506-11.

[23] Baby TT, Ramaprabhu S. Experimental investigation of the thermal transport properties of a carbon nanohybrid dispersed nanofluid. Nanoscale. 2011;3(5):2208-14.

[24] Sandhya M, Ramasamy D, Sudhakar K, Kadirgama K, Samykano M, Harun WS, Najafi G, Mofijur M, Mazlan M. A systematic review on graphene-based nanofluids application in renewable energy systems: Preparation, characterization, and thermophysical properties. Sustainable Energy Technologies and Assessments. 2021 Apr 1;44:101058.

[25] Sandhya M, Ramasamy D, Sudhakar K, Kadirgama K, Harun WS. Heat transfer performance of a radiator with and without louvered strip by using Graphene-based nanofluids. Journal of Thermal Engineering. (2021) Sep;7(6).

[26] Novoselov KS, Geim AK, Morozov SV, Jiang DE, Zhang Y, Dubonos SV, Grigorieva IV, Firsov AA. Electric field effect in atomically thin carbon films. science. 2004 Oct 22;306(5696):666-9.

[27] Sandhya M, Ramasamy D, Kadirgama K, Harun WS, Samykano M, Ameer A. Enhancement of tribological behaviour and thermophysical properties of engine oil lubricant by Graphene/Co-Cr nanoparticle additives for preparation of stable nanolubricant. InIOP

Conference Series: Materials Science and Engineering 2021 Feb 1 (Vol. 1078, No. 1, p. 012016). IOP Publishing.

[28] Sandhya M, Ramasamy D, Sudhakar K, Kadirgama K, Harun WS. Ultrasonication an intensifying tool for preparation of stable nanofluids and study the time influence on distinct properties of graphene nanofluids–A systematic overview. Ultrasonics sonochemistry. 2021 May;73.

[29] Teng CC, Ma CC, Lu CH, Yang SY, Lee SH, Hsiao MC, Yen MY, Chiou KC, Lee TM. Thermal conductivity and structure of non-covalent functionalized graphene/epoxy composites. Carbon. 2011 Dec 1;49(15):5107-16.

[30] Sandhya, M., Ramasamy, D., Sudhakar, K., Kadirgama, K., & Harun, W. (2021). Enhancement of the heat transfer in radiator with louvered fin by using Graphene-based hybrid nanofluids. Paper presented at the IOP Conference Series: Materials Science and Engineering.

[31] Sarsam WS, Amiri A, Kazi SN, Badarudin A. Stability and thermophysical properties of non-covalently functionalized graphene nanoplatelets nanofluids. Energy conversion and management. 2016 May 15;116:101-11.

[32] Sani E, Mercatelli L, Barison S, Pagura C, Agresti F, Colla L, Sansoni P. Potential of carbon nanohorn-based suspensions for solar thermal collectors. Solar Energy Materials and Solar Cells. 2011 Nov 1;95(11):2994-3000.

[33] Luo Z, Wang C, Wei W, Xiao G, Ni M. Performance improvement of a nanofluid solar collector based on direct absorption collection (DAC) concepts. International Journal of Heat and Mass Transfer. 2014 Aug 1;75:262-71.

[34] Sani E, Barison S, Pagura C, Mercatelli L, Sansoni P, Fontani D, Jafrancesco D, Francini F. Carbon nanohorns-based nanofluids as direct sunlight absorbers. Optics Express. 2010 Mar 1;18(5):5179-87.

[35] Geim AK, Novoselov KS. The rise of Graphene. InNanoscience and technology: a collection of reviews from nature journals 2010 (pp. 11-19).

[36] Sandhya M, Ramasamy D, Sudhakar K, Kadirgama K, Harun WS. Enhancement of the heat transfer in radiator with louvered fin by using Graphene-based hybrid nanofluids. In IOP Conference Series: Materials Science and Engineering (2021) Feb 1 (Vol. 1062, No. 1, p. 012014). IOP Publishing.

[37] Vakili M, Hosseinalipour SM, Delfani S, Khosrojerdi S. Photothermal properties of graphene nanoplatelets nanofluid for low-temperature direct absorption solar collectors. Solar Energy Materials and Solar Cells. 2016 Aug 1;152:187-91.

[38] Sani E, Vallejo JP, Cabaleiro D, Lugo L. Functionalized graphene nanoplatelet-nanofluids for solar thermal collectors. Solar Energy Materials and Solar Cells. 2018 Oct 1;185:205-9.

[39] Abd Malek MN, Hussin NM, Embong NH, Bhuyar P, Rahim MH, Govindan N, Maniam GP. Ultrasonication: a process intensification tool for methyl ester synthesis: a mini review. Biomass Conversion and Biorefinery. 2020 Oct 25:1-1.

[40] Abd Malek MN, Pushparaja L, Hussin NM, Embong NH, Bhuyar P, Rahim MH, Maniam GP. Exploration of efficiency of nano calcium oxide (CaO) as catalyst for enhancement of biodiesel production. Journal of microbiology, biotechnology and food sciences. 2021 Apr 7:e3935-.

[41] Sandhya M, Ramasamy D, Kadirgama K, Harun WS, Samykano M, Ameer A. Enhancement of tribological behaviour and thermophysical properties of engine oil lubricant by Graphene/Co-Cr nanoparticle additives for preparation of stable nanolubricant. In IOP Conference Series: Materials Science and Engineering (2021) Feb 1 (Vol. 1078, No. 1, p. 012016). IOP Publishing.

[42] Chakraborty S, Panigrahi PK. Stability of nanofluid: A review. Applied Thermal Engineering. 2020 Jun 25;174:115259.

[43] Batakliev T, Petrova-Doycheva I, Angelov V, Georgiev V, Ivanov E, Kotsilkova R, Casa M, Cirillo C, Adami R, Sarno M, Ciambelli P. Effects of graphene nanoplatelets and multiwall carbon nanotubes on the structure and mechanical properties of poly (lactic acid) composites: a comparative study. Applied Sciences. 2019 Jan;9(3):469.

[44] Gutić S, Dobrota AS, Gavrilov N, Baljozović M, Pašti IA, Mentus SV. Surface charge storage properties of selected graphene samples in pH-neutral aqueous solutions of alkali metal chlorides-particularities and universalities. Int. J. Electrochem. Sci. 2016 Oct 1;11(10):8662-82.

[45] Rashad M, Pan F, Tang A, Lu Y, Asif M, Hussain S, She J, Gou J, Mao J. Effect of graphene nanoplatelets (GNPs) addition on strength and ductility of magnesium-titanium alloys. Journal of Magnesium and alloys. 2013 Sep 1;1(3):242-8.

[46] He P, Gu H, Wang G, Yang S, Ding G, Liu Z, Xie X. Kinetically enhanced bubble-exfoliation of graphite toward high-yield preparation of high-quality Graphene. Chemistry of Materials. 2017 Oct 24;29(20):8578-82.

[47] Soo M, Mi X, Goroshin S, Higgins AJ, Bergthorson JM. Combustion of particles, agglomerates, and suspensions–A basic thermophysical analysis. Combustion and Flame. 2018 Jun 1;192:384-400.

[48] Mehrali M, Sadeghinezhad E, Latibari ST, Kazi SN, Mehrali M, Zubir MN, Metselaar HS. Investigation of thermal conductivity and rheological properties of nanofluids containing graphene nanoplatelets. Nanoscale research letters. 2014 Dec;9(1):1-2.

[49] Singh P, Campidelli S, Giordani S, Bonifazi D, Bianco A, Prato M. Organic functionalization and characterization of single-walled carbon nanotubes. Chemical Society Reviews. 2009;38(8):2214-30.

[50] Liu WW, Chai SP, Mohamed AR, Hashim U. Synthesis and characterization of graphene and carbon nanotubes: A review on the past and recent developments. Journal of Industrial and Engineering Chemistry. 2014 Jul 25;20(4):1171-85.

[51] Căldăraru M, Sprinceana D, Popa VT, Ionescu NI. Surface dynamics in tin dioxide-containing catalysts II. Competition between water and oxygen adsorption on polycrystalline tin dioxide. Sensors and Actuators B: Chemical. 1996 Jan 1;30(1):35-41.

[52] Madejová J, Barlog M, Jankovič Ľ, Slaný M, Pálková H. Comparative study of alkylammonium-and alkylphosphonium-based analogues of organo-montmorillonites. Applied Clay Science. 2021 Jan 1;200:105894.

[53] Slaný M, Jankovič Ľ, Madejová J. Structural characterization of organo-montmorillonites prepared from a series of primary alkylamines salts: Mid-IR and near-IR study. Applied Clay Science. 2019 Aug 1;176:11-20.

[54] El-Wakil NA, Hassan ML. Structural changes of regenerated cellulose dissolved in FeTNa, NaOH/thiourea, and NMMO systems. Journal of Applied Polymer Science. 2008 Sep 5;109(5):2862-71.

[55] Du W, Slaný M, Wang X, Chen G, Zhang J. The inhibition property and mechanism of a novel low molecular weight zwitterionic copolymer for improving wellbore stability. Polymers. 2020 Mar;12(3):708.

570 [56] Adsul M, Soni SK, Bhargava SK, Bansal V. Facile approach for the dispersion of regenerated
571 cellulose in aqueous system in the form of nanoparticles. Biomacromolecules. 2012 Sep
572 10;13(9):2890-5.
573 [57] Zhang L, Ruan D, Zhou J. Structure and properties of regenerated cellulose films prepared
574 from cotton linters in NaOH/urea aqueous solution. Industrial & Engineering Chemistry
575 Research. 2001 Dec 12;40(25):5923-8.
576 [58] Yadav SK, Cho JW. Functionalized graphene nanoplatelets for enhanced mechanical and
577 thermal properties of polyurethane nanocomposites. Applied surface science. 2013 Feb
578 1;266:360-7.
579 [59] Hereijgers J, Desmet G, Breugelmans T, De Malsche W. Strategies to integrate porous layers
580 in microfluidic devices. Microelectronic Engineering. 2015 Jan 25;132:1-3.
581 [60] Aravind SJ, Baskar P, Baby TT, Sabareesh RK, Das S, Ramaprabhu S. Investigation of
582 structural stability, dispersion, viscosity, and conductive heat transfer properties of
583 functionalized carbon nanotube based nanofluids. The Journal of Physical Chemistry C.
584 2011 Sep 1;115(34):16737-44.
585 [61] Huang M, Borzoei H, Abdollahi A, Li Z, Karimipour A. Effect of concentration and
586 sedimentation on boiling heat transfer coefficient of GNPs-SiO2/deionized water hybrid
587 Nanofluid: An experimental investigation. International Communications in Heat and
588 Mass Transfer. 2021 Mar 1;122:105141.
589 [62] Sadri R, Hosseini M, Kazi SN, Bagheri S, Zubir N, Ahmadi G, Dahari M, Zaharinie T. A
590 novel, eco-friendly technique for covalent functionalization of graphene nanoplatelets and
591 the potential of their nanofluids for heat transfer applications. Chemical Physics Letters.
592 2017 May 1;675:92-7.
593 [63] Benedict, F., Kumar, A., Kadirgama, K., Mohammed, H.A., Ramasamy, D., Samykano, M.
594 and Saidur, R., 2020. Thermal performance of hybrid-inspired coolant for radiator
595 application. Nanomaterials, 10(6), p.1100.
596 [64] Tantra R, Schulze P, Quincey P. Effect of nanoparticle concentration on zeta-potential
597 measurement results and reproducibility. Particuology. 2010 Jun 1;8(3):279-85.
598 [65] Dukhin SS, Kretzschmar G, Miller R. Dynamics of adsorption at liquid interfaces: theory,
599 experiment, application. Elsevier; 1995 Apr 11.

[66] Sennett P, Olivier JP. Colloidal dispersions, electrokinetic effects, and the concept of zeta potential. Industrial & Engineering Chemistry. 1965 Aug 1;57(8):32-50.

[67] Ostolska I, Wiśniewska M. Application of the zeta potential measurements to explanation of colloidal Cr 2 O 3 stability mechanism in the presence of the ionic polyamino acids. Colloid and polymer science. 2014 Oct;292(10):2453-64.

[68] Xu X, Yu Z, Zhu Y, Wang B. Effect of sodium oleate adsorption on the colloidal stability and zeta potential of detonation synthesized diamond particles in aqueous solutions. Diamond and related materials. 2005 Feb 1;14(2):206-12.